

Research Article

Preformulation Stability Studies of the New Dipeptide Angiotensin-Converting Enzyme Inhibitor RS-10029

Leo Gu^{1,2} and Robert G. Strickley¹

Received March 29, 1988; accepted June 27, 1988

The degradation kinetics, products, and mechanisms of RS-10029 (2), 2-[2-[(1-carboxylic acid)-3-phenylpropyl]amino-1-oxopropyl]-6,7-dimethoxy-1,2,3,4-tetrahydroisoquinoline-3-carboxylic acid (S,S,S), in aqueous solutions from pH 1 to pH 13 were studied at 50, 60, and 80°C. Pseudo-first-order kinetics were obtained throughout the entire pH range studied, and the log(rate)-pH profile reflected four kinetic processes (k_o , k'_o , k''_o , and k_{OH}) as well as the three pK_a 's of 2. Excellent mass balance (>96%) was obtained for the four major products 3-6 throughout the entire pH range studied even though four other minor products can be detected by high-performance liquid chromatography (HPLC). At pH 8.0 and below, intramolecular aminolysis leading to diketopiperazine (DKP) 5 accounted for greater than 65% of the neutral or water-catalyzed (k_o and k'_o) processes. Amide hydrolysis leading to products 3 and 4 and epimerization of DKP 5 to the (R,S,S) diastereomer 6 accounted for the remaining 35% of the neutral or water catalyzed processes. At pH values above 8.0, DKP 5 formation begins to decrease as the amide hydrolysis increases so that both mechanisms account for the neutral or water-catalyzed k''_o process. Above pH 11.0 amide hydrolysis dominates and is responsible for the specific base-catalyzed (k_{OH}) process. The four minor products detected by HPLC are two diastereomers (7 and 8) of 2 and the two diastereomers (9 and 10) of the DKP 5. The stability results between 2 and its ester prodrug (1) are compared.

KEY WORDS: angiotensin-converting enzyme (ACE) inhibitor; RS-10029; degradation; products; peptides.

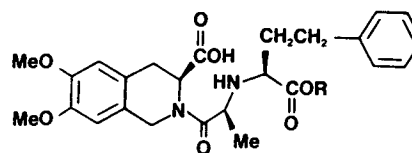
INTRODUCTION

RS-10029 (2), 2-[2-[(1-carboxylic acid)-3-phenylpropyl]amino-1-oxopropyl]-6,7-dimethoxy-1,2,3,4-tetrahydroisoquinoline-3-carboxylic acid, is the active form of RS-10085 (1) (1,2) (Scheme I) to be developed as a dipeptide angiotensin-converting enzyme (ACE) inhibitor (3,4). In a previous report we have disclosed the aqueous stability of ester prodrug 1 (5); the facile diketopiperazine (DKP) formation and ester hydrolysis of 1 have resulted in an estimated aqueous shelf life (time to reach 90% remaining) of only ~2 months at the pH of maximum stability, 4.5. It is therefore important to study the stability of 2 in aqueous solution at the preformulation stage to facilitate the design of an iv formulation. Also, since ester hydrolysis is not feasible for 2, it is of interest to examine the importance of pH (6) and amino pK_a effects on the DKP formation of 2.

MATERIALS AND METHODS

Chemicals

RS-10085 (1), RS-10029 (2), compounds 3 and 4, DKP of RS-10029 (5), and RSS and SSR isomers of RS-10029 (7 and



1 RS-10085 (S,S,S); R = Et
2 RS-10029 (S,S,S); R = H

Scheme I

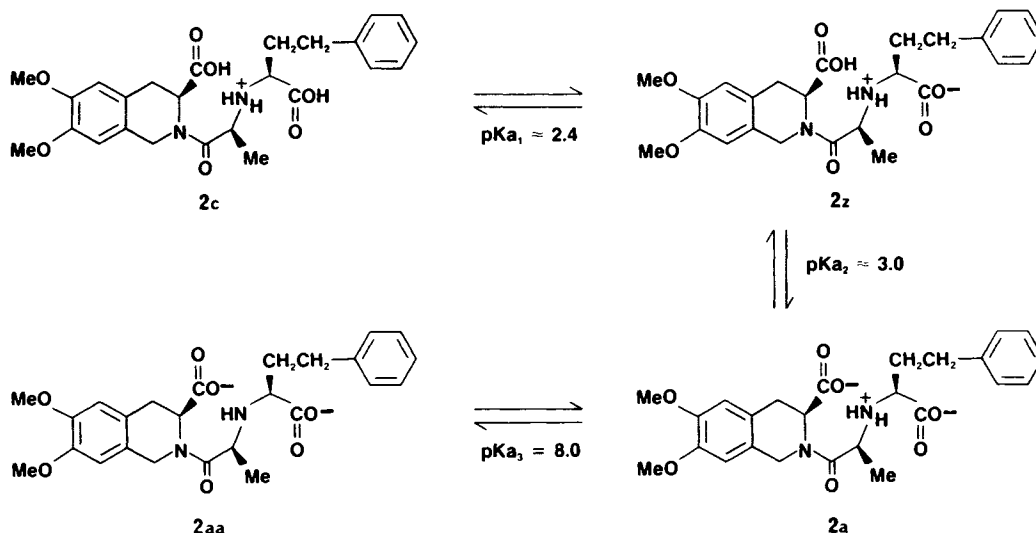
8) were obtained from the Institute of Organic Chemistry, Syntex Research. High-performance liquid chromatography (HPLC)-grade acetonitrile and tetrahydrofuran and nano-pure water were used to prepare the mobile phase. All other chemicals were analytical grade and used as received.

Instrumentation

A Radiometer Model PHM64 Research pH meter equipped with a Radiometer Model GK2410C combination electrode was used to measure the pH of the solution. HPLC was performed using an Altex Model 110 pump equipped with a Kratos 757 variable-wavelength UV detector, a Micromeritics 728 autosampler, and a Spectra-Physics 4100 computing integrator. A Hewlett-Packard HP 1090 system was used for the gradient analysis.

¹ Institute of Pharmaceutical Sciences, Syntex Research, Palo Alto, California 94304.

² To whom correspondence should be addressed.



Scheme II

pH-Solubility Profile

The solubility of **2** in water as a function of the pH was determined by first adding an excess amount of drug to ~10 ml of nanopure water at 25°C and stirring vigorously for at least 30 min. The temperature was controlled by keeping the mixture in a thermal-jacketed beaker. Solubilities at pH values, less than that of the saturated solution, were determined by adding 1.0 M HCl to adjust the pH. After each addition, equilibration (or constant solubility) was attained after 30 min of stirring. A 0.5-ml aliquot was withdrawn, then filtered through a 0.45 μm Millipore filter, and the pH of the filtrate

was measured. The filtrate was then diluted with mobile phase and assayed by HPLC.

pK_a Titration Method

In a typical titration experiment approximately 19.5 mg of accurately weighed **2** (1.04 mM) was added to 40.0 ml of water in a thermal-jacketed beaker equilibrated at the desired temperature. With constant stirring and nitrogen purging, the drug solution was titrated with a 0.0105 M standard KOH solution. The pH was measured and the pK_{a3} determined using the method for a typical monoacidic base (7).

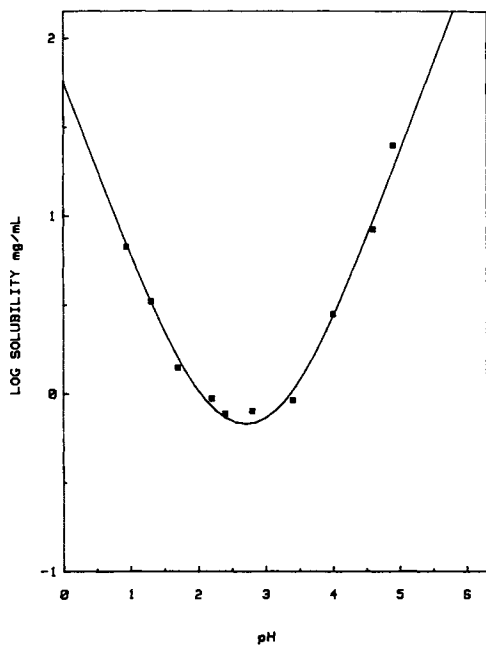


Fig. 1. Aqueous solubility of **2** as a function of pH at 25°C. The solid line is the theoretical curve defined by the relationship $S_{\text{obs}} = S_i / (1 + [\text{H}^+]/K_{a1} + K_{a2}/[\text{H}^+])$, where $S_i = 0.30$ mg/ml, $K_{a1} = 4.0 \times 10^{-3}$, and $K_{a2} = 7.9 \times 10^{-4}$. The data points were obtained experimentally.

HPLC Methods

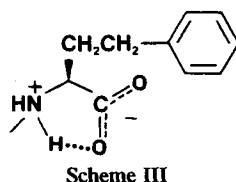
Two (an isocratic and a gradient) stability-specific reverse-phase HPLC methods have been developed for the quantitation of RS-10029. Both methods employ an Altex Ultrasphere-ODS 5- μm 4.6 \times 250-mm column, a flow rate of 1.0 ml/min, and UV detection at 215 nm. The isocratic method employs a mobile phase of (65/30/5) 0.05 M $\text{NH}_4\text{H}_2\text{PO}_4$ (pH 2.0)/ CH_3CN /THF and gives excellent linear responses ($r = 0.99998$) with injection sizes of RS-10029 in the range of 0.06 to 4.6 μg . The gradient method used mainly for mass balance studies employs a mobile phase of 0.05 M $\text{NH}_4\text{H}_2\text{PO}_4$ (pH 2.0)/ CH_3CN from an 85/15 ratio at time 0 to a 40/60 ratio at time 30 min. Excellent linearity ($r = 0.9998$) was also obtained for the gradient method in the range of 0.06 to 4.6 μg injected. The stability specificity of both meth-

Table I. The Dissociation Constants (pK_a) of **1** in Aqueous Solution

Temperature (°C)	pK _{a1} ^a	pK _{a2} ^a	pK _{a3} ^b
25	2.4	3.3	7.97
50	—	—	7.60
60	—	—	7.49
80	—	—	7.22

^a Determined by the solubility method [Eq. (1)].

^b Determined by potentiometric titration.



ods was supported by the complete disappearance of 2 when totally degraded samples were injected.

Kinetic Methods

Acetate, phosphate, and carbonate buffer solutions containing a 0.010 *M* total buffer concentration were freshly prepared before use and KCl was added to adjust the total ionic strength to 0.10 *M*. The pH of each buffer solution was measured at the reaction temperature. For very acidic and basic solutions, aqueous HCl and KOH solutions were used to obtain the desired pH.

In a typical kinetic experiment, 1.5-ml aliquots of the buffer solution containing 20–50 $\mu\text{g/ml}$ of RS-10029 were transferred to prewashed 2-ml Type I amber glass ampoules. The ampoules were then flame-sealed and stored in a 50, 60, or 80°C oven until predetermined time periods, when the ampoules were removed and quenched to 0°C in an ice bath. The samples were allowed to warm to room temperature before assaying by HPLC.

RESULTS AND DISCUSSION

Four major forms of 2 exist in solution: the cation (2c), the zwitterion (2z), the anion (2a), and the doubly charged anion (2aa) reflecting the pK_{a_1} , pK_{a_2} , and pK_{a_3} of the drug (Scheme II).

In order to determine the carboxylic acid pK_{a_1} and pK_{a_2} values, the pH–solubility profile was established as shown in Fig. 1. The equation for the total solubility (S_{obs}) of the drug

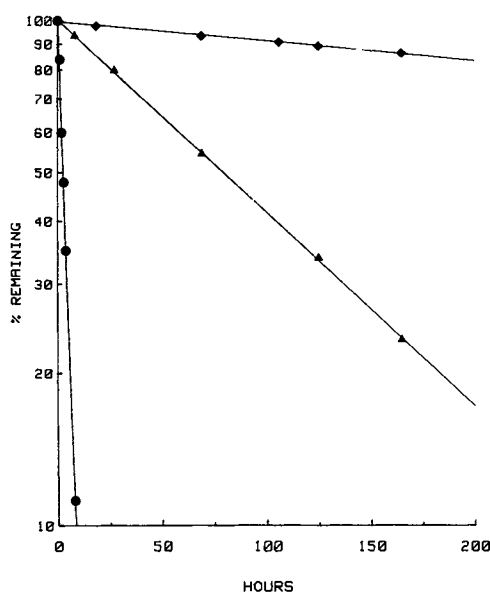


Fig. 2. Pseudo-first-order kinetics of the degradation of 2 in aqueous solution at 80°C. (●) pH 2.1; (▲) pH 5.2; (◆) pH 10.5.

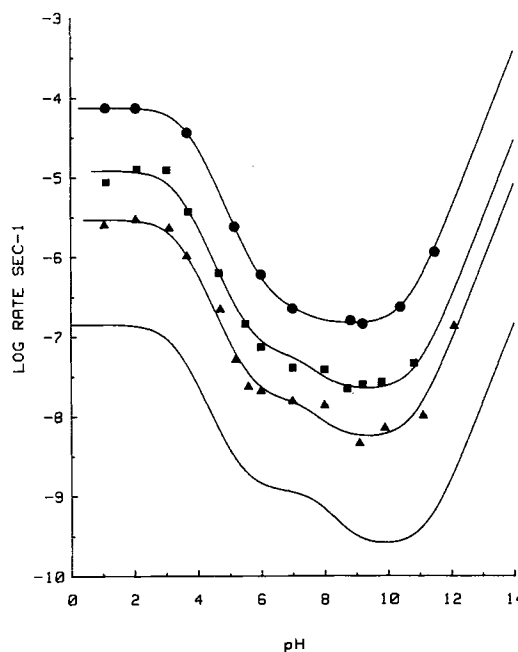


Fig. 3. Log (rate)–pH profiles for the degradation of 2 in aqueous solution at 50°C (▲), 60°C (■), and 80°C (●). The solid lines are the nonlinear regression fit using Eq. (2). The line without data points is the calculated profile at 25°C using the rate data (Table II) and the activation parameters (Table III).

as a function of pH which applies is given by (7)

$$S_{\text{obs}} = S_1 (1 + [\text{H}^+]/K_{a_1} + K_{a_2}/[\text{H}^+]) \quad (1)$$

where S_1 is the saturated solubility of the zwitterion, 2z ($S_1 = 0.30 \text{ mg/ml}$). The pK_a values that gave the best fit to Eq. (1) were $pK_{a_1} = 2.4$ and $pK_{a_2} = 3.1$ (Table I). The carboxylic acid attached to the third chiral center (counting from left to right) is assigned to have the pK_{a_1} value because it is adjacent to the ammonium group, which can provide both an electron-withdrawing effect and an intramolecular hydrogen bonding capability (Scheme III). The values of the pK_{a_1} and pK_{a_2} may be assumed to be unaffected by temperature as is the pK_a of the carboxylic acid in 1 (5) and in most other carboxylic acids (7).

Since the solubility of 2 exceeds 150 mg/ml at pH's above 5.5, the amine pK_{a_3} was determined by potentiometric titration and the results are summarized in Table I. The pK_{a_3} decreased as the temperature increased, consistent with that expected for a typical amine (7). At 25°C the amine pK_{a_3} value of 2 (= 8.0) is much greater than the amino pK_a of 1 (= 5.4). This can be attributed partially to the stronger base weakening group of the ester in 1 than the carboxylate (attached to the third chiral center) in 2 (7) and partially to the intramolecular hydrogen bonding between the ammonium and the carboxylate groups in 2 (Scheme III).

Kinetics

The aqueous stability of RS-10029 was studied in buffered solutions from pH 1 to pH 13 at 50, 60, and 80°C. The degradation kinetics were followed by an isocratic stability-specific HPLC method (see Materials and Methods) and were found to be strictly first order down to four half-lives.

Table II. Effect of Temperature on the Apparent Rate Constants for the Degradation of 2 in Aqueous Solution

Temperature (°C)	Rate constant ^a			
	k_o (sec ⁻¹)	k'_o (sec ⁻¹)	k''_o (sec ⁻¹)	k_{OH} (M ⁻¹ sec ⁻¹)
80	7.39×10^{-5}	2.54×10^{-7}	1.46×10^{-7}	1.30×10^{-5}
60	1.18×10^{-5}	4.77×10^{-8}	2.46×10^{-8}	3.40×10^{-6}
50	2.88×10^{-6}	1.67×10^{-8}	5.33×10^{-9}	1.43×10^{-6}
25 ^b	1.37×10^{-7}	1.20×10^{-9}	2.53×10^{-10}	1.71×10^{-7}

^a Obtained from a nonlinear least-squares fit of the rate data (Fig. 2) to Eq. (3).

^b Extrapolated using the Arrhenius parameters given in Table III.

Since very low buffer concentrations were used (0.01 M), no correction for possible buffer catalysis was made.

Typical first-order plots at 80°C and pH 2.1, 5.2, and 10.5 are shown in Fig. 2. The influence of pH on the degradation kinetics of 2 can best be depicted by the log (rate)–pH profile given in Fig. 3, in which the logarithm of the observed rate constants (K_{obs}) is plotted against the pH. The rate profile reached a plateau at pH values below 3, indicating that the cation 2c and the zwitterion 2z may have similar reactivities. Thus, although other kinetically equivalent systems cannot be ruled out, the shape of the pH–rate profiles in Fig. 3 can be explained by the occurrence of neutral or water-catalyzed processes of the cation 2c and zwitterion 2z (k_o), anion 2a (k'_o), and dianion 2aa (k''_o), respectively, and a specific base-catalyzed (k_{OH}) process of the dianion 2aa according to the expression,

$$\text{rate} = k_{obs} [2]_t \quad (2)$$

and

$$k_{obs} = k_o(a_H^3/x + K_{a_1}a_H^2/x) + k'_o(K_{a_1}K_{a_2}a_H/x) + (k''_o + k_{OH}a_{OH})(K_{a_1}K_{a_2}K_{a_3}/x) \quad (3)$$

where $x = a_H^3 + K_{a_1}a_H^2 + K_{a_1}K_{a_2}a_H + K_{a_1}K_{a_2}K_{a_3}$

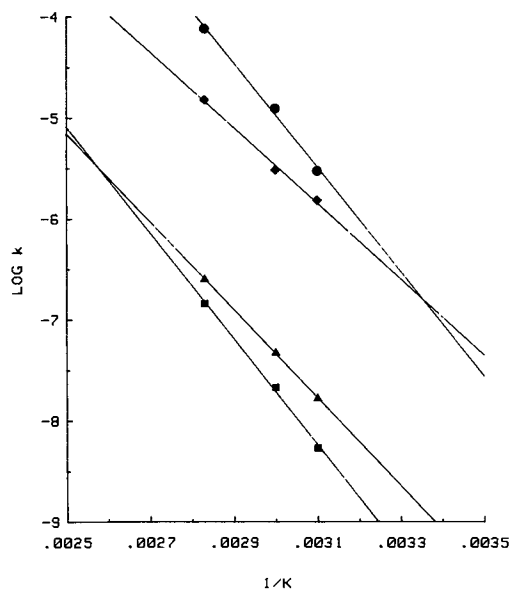


Fig. 4. Arrhenius plots of the degradation of 2. The rate constants k_o (●), K'_o (▲), k''_o (■), and k_{OH} (◆) are taken from Table II.

In Eq. (3), $[2]_t$ is the total concentration of the drug at time t , and a_H^3/x , $K_{a_1}a_H^2/x$, $K_{a_1}K_{a_2}a_H/x$, and $K_{a_1}K_{a_2}K_{a_3}/x$ are, respectively, the fractions of 2c, 2z, 2a, and 2aa. The a_H and a_{OH} are, respectively, the hydrogen and hydroxide ion activity at the reaction temperature. The values of the apparent rate constants at different temperatures were determined using Eq. (3), the K_{a_1} , and K_{a_2} , and K_{a_3} values listed in Table I, and a nonlinear regression analysis method (8). The curves drawn in Fig. 3 were constructed using the apparent rate constants summarized in Table II. The apparent rate constants listed in Table II were found to obey the Arrhenius equation (Fig. 4) and the corresponding activation energies, entropies, and enthalpies derived are listed in Table III. The values of the apparent rate constants extrapolated to 25°C (Table II) were substituted into Eq. (3) giving the pH–log (rate) profile at 25°C (Fig. 3). The results predict a ≥ 2 -year shelf life at pH values between 6.0 and 12.0.

Product Distribution and Mechanisms of Degradation

A total of eight degradation products in aqueous solution have been detected and identified by the gradient HPLC method (Scheme IV). A chromatogram showing all of these peaks at pH 7.2 and 40% remaining is given in Fig. 5. The structure assignment of these eight products was achieved by the HPLC coelution method. Authentic samples of the RSS and SSR drug isomers (7 and 8), the two amide hydrolysis products (3 and 4), and the cyclization product, DKP 5, were available for the study. (RSS) and (SSR) drug DKP isomers (6 and 9) were prepared *in solution* by degrading, respectively, (RSS) and (SSR) drug isomer in 0.01 N HCl under the conditions reported previously (5). The potential formation of (SRS) drug isomer and (SRS) drug DKP isomer cannot be determined in a similar way due to the lack of authentic (SRS) isomer of 2.

Table III. Summary of Activation Parameters for the Degradation of 2 in Aqueous Solution

Constant	E_a (kcal mol ⁻¹)	logA	ΔH (kcal mol ⁻¹)	ΔS (cal mol ⁻¹ K ⁻¹)
k_o	24.1 ± 2.2	10.8 ± 1.5	23.5 ± 2.2	-11.1 ± 2.1
k'_o	20.4 ± 0.7	6.06 ± 0.5	19.8 ± 0.8	-32.9 ± 5.2
k''_o	24.5 ± 3.1	8.36 ± 2.0	23.8 ± 3.1	-22.4 ± 8.3
k_{OH}	16.6 ± 0.7	5.4 ± 0.5	15.9 ± 0.7	-36.0 ± 7.2

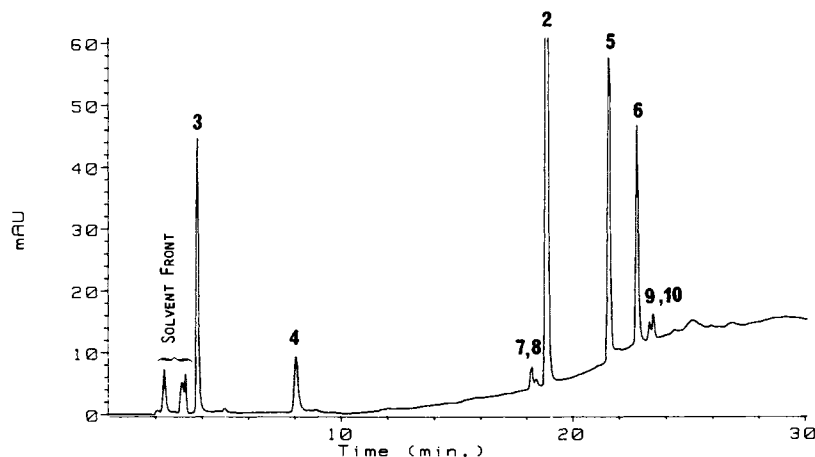


Fig. 5. An HPLC chromatogram showing the separation of degradation products 3–10 from the drug peak 2.

The material balance for the reaction determined by HPLC response factors for products 3–6 was found to be excellent and exceeded 96% in all cases. The product distribution is similar at different temperatures but varied greatly with the pH of the solution. The product distribution as a function of pH at 60°C and about 80% remaining is presented in Fig. 6. At pH values of 8.0 or below the DKP 5 and DKP 6 accounted for 67–96% of the observed degradation, and the two hydrolysis products, 3 and 4, accounted for most of the remaining products. Also, at a given pH, the product ratio of 5/6 decreased as the extent of the reaction increased, while the total percentage of these two products remained unchanged, indicating that DKP 6 comes from the epimerization of the primary product DKP 5. Thus, intramolecular aminolysis is responsible for the majority of the neutral or water-catalyzed kinetic processes (k_o and k'_o), with amide hydrolysis responsible for the remaining mechanism of the degradation. Taking into account the hydrolysis portion from the product analysis, the cyclization portion of the k_o term for 2 at 60 or 80°C is similar to (~0.8-fold) that of 1 at 60 or 80°C, while the cyclization portion of the k'_o term of 2, on the other hand, was ~10-fold smaller than the k'_o term for 1 (Table IV).

According to Scheme II, the major species present in

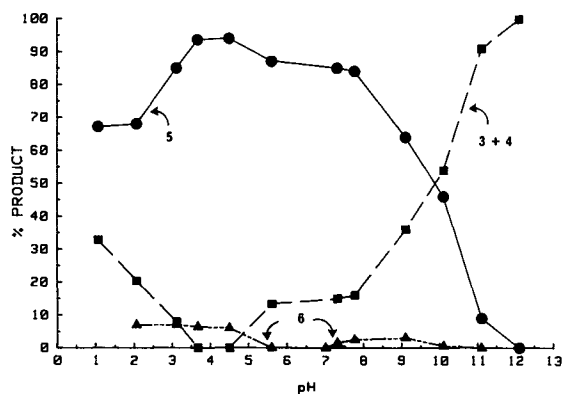


Fig. 6. The distribution of the degradation products 3–6 as a function of pH at 50°C and ~80% remaining.

aqueous solution at pH values below 8 are 2c and 2z and 2a. Like that suggested for the DKP formation of 1 (5), the tautomers, 2c' and 2z' and 2a' are probably the reactive intermediates (9) for the neutral or water-catalyzed cyclization processes k_o and k'_o , respectively (Scheme V). Since the amino group is more basic in 2 ($pK_a = 8.0$) than in 1 ($pK_a = 5.4$), the microscopic cyclization constants of the tautomers (k_i and k'_i) should be greater for the former. The same basicity argument, however, would suggest that the equilibrium constants (K_o and K'_o) be smaller for 2 than those for 1. These two effects apparently are canceled by each other for the k_o process of 2, but the smaller K'_o must be the dominant factor to account for the ~10-fold smaller k'_o term of 2 as compared to that of 1.

Amide hydrolysis products 3 and 4 increase from ~0% at pH 5.0 to 35% at pH 1.0, indicating the importance of a specific acid-catalyzed hydrolysis process. This is somewhat unexpected, as similar amide hydrolysis was not observed for 1 at pH values below 4.0 (5). One possible reason could be that the higher amino pK_{a_3} (=8.0) of 2 provided more electron withdrawing effect on the amide bond, thus facilitating the hydrolysis.

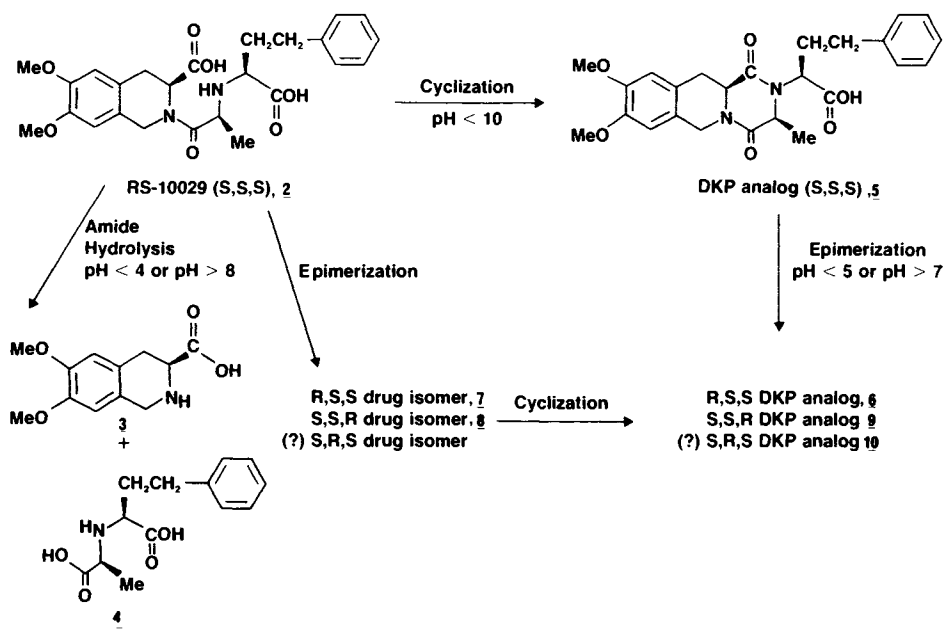
Above pH 8.0, DKP formation begins to decrease as the hydrolysis mechanism begins to increase such that at a pH of about 10 both degradation pathways compete equally (Fig. 6). Above pH 11.0, hydrolysis dominates and accounts for $\geq 90\%$ of the degradation, with DKP 5 and a small amount of

Table IV. Cyclization Rate Comparisons Between 1 and 2 at 60 and 80°C

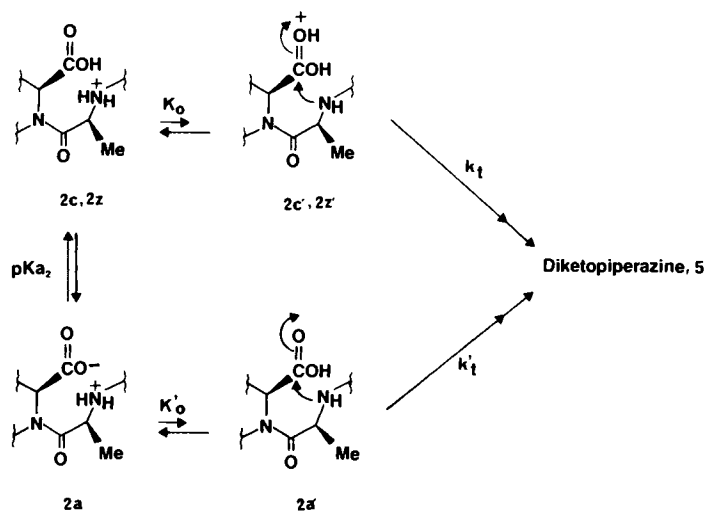
Substrate	Temp. (°C)	k_o (cyc), sec^{-1a}	Rate ratio	k'_o (cyc), sec^{-1a}	Rate ratio
1 ^b	80	6.52×10^{-5}	1	1.61×10^{-6}	1
2	80	4.95×10^{-5}	0.76	1.57×10^{-7}	0.098
1 ^b	60	9.60×10^{-6}	1	3.14×10^{-7}	1
2	60	7.91×10^{-6}	0.82	3.15×10^{-8}	0.10

^a Cyclization rate constant calculated from the respective rate constant and product studies.

^b Calculated from data presented in Ref. 5.



Scheme IV



Scheme V

epimerization of **2** (only about 4% of the observed degradation in 0.1 N KOH is epimerization) accounting for the remainder of the degradation. Thus both intramolecular aminolysis and amide hydrolysis are responsible for the neutral or water-catalyzed k'_{\circ} process, but amide hydrolysis accounts for most ($\geq 95\%$) of the specific base-catalyzed k_{OH} process.

CONCLUSION

Through detailed kinetic and product distribution analysis, the major degradation mechanisms of **2** in aqueous solutions were determined. The higher amino $\text{p}K_{\text{a}_2}$ of **2**, as compared to that of **1**, resulted in a facile amide hydrolysis process at low pH values and a slower k'_{\circ} term for the cyclization process at intermediate pH values. The latter effect is beneficial especially for the formulation development, as a greater than 2-year shelf life of **2** can be obtained in aqueous solution at 25°C.

REFERENCES

1. S. Klutchko, C. J. Blankley, R. W. Fleming, J. M. Hinkley, A. E. Werner, I. Nordin, A. Holmes, M. L. Hoefle, D. M. Cohen, A. D. Essenburg, and H. R. Kaplan. *J. Med. Chem.* **29**:1953-1961 (1986).
2. D. M. Cohen, A. D. Essenburg, B. J. Olszewski, R. M. Singer, M. J. Ryan, D. B. Evans, and H. R. Kaplan. *Pharmacologist* **26**:266 (1984).
3. M. J. Wyvratt and A. A. Patchett. *Med. Res. Rev.* **5**:485-531 (1985).
4. M. A. Weber and R. M. Zusman. *Drug Ther.* 43-54 (1986).
5. L. Gu, and R. G. Strickley. *Pharm. Res.* **4**:392-397 (1987).
6. R. E. Bouvette and G. A. Digenis. *Pharm. Res.* **4**:S-35 (1987).
7. A. Albert and E. P. Serjeant. In *The Determination of Ionization Constants*, 2nd ed., Chapman and Hall, London, 1971.
8. P. R. Bevington. In *Data Reduction and Error Analysis for the Physical Sciences*, McGraw-Hill, New York, 1969.
9. A. A. Brewerton, D. A. Long, and T. G. Truscott. *Trans. Faraday Soc.* **66**:2297-2304 (1970).